Evaluation of Different Synchrotron Beam Line Configurations for X-ray Fluorescence Analysis of Environmental Samples.

ARTICLE *in* ANALYTICAL CHEMISTRY · JULY 2014

Impact Factor: 5.64 · DOI: 10.1021/ac5016535 · Source: PubMed

4 AUTHORS, INCLUDING:

Sean Richard Barberie
University of Alaska Fairbanks
3 PUBLICATIONS **5** CITATIONS

SEE PROFILE

C. F. Cahill
University of Alaska System
42 PUBLICATIONS **189** CITATIONS

SEE PROFILE

analytical chemistry

Article

pubs.acs.org/ac

Evaluation of Different Synchrotron Beamline Configurations for X-ray Fluorescence Analysis of Environmental Samples

Sean R. Barberie,[†] Christopher R. Iceman,[†] Catherine F. Cahill,[†] and Thomas M. Cahill*[,‡]

[†]Department of Chemistry and Biochemistry, University of Alaska Fairbanks, 900 Yukon Drive, Room 194, Fairbanks, Alaska 99775-6160, United States

[‡]School of Mathematical and Natural Sciences, Arizona State University at the West Campus, P.O. Box 37100, Phoenix, Arizona 85069, United States

ABSTRACT: Synchrotron radiation X-ray fluorescence (SR-XRF) is a powerful elemental analysis tool, yet synchrotrons are large, multiuser facilities that are generally not amenable to modification. However, the X-ray beamlines from synchrotrons can be modified by simply including X-ray filters or removing monochromators to improve the SR-XRF analysis. In this study, we evaluated four easily applied beamline configurations for the analysis of three representative environmental samples, namely a thin aerosol sample, an intermediate thickness biological sample, and a thick rare earth mineral specimen. The results showed that the "white beam" configuration, which was simply the full, polychromatic output of the synchrotron, was the optimal configuration for the analysis of thin samples with little mass. The "filtered white beam" configuration removed the lower energy X-rays from the excitation beam so it gave better sensitivity for elements emitting more energetic X-rays. The "filtered white beam−filtered detector" configuration sacrifices the lower energy part of the spectrum (<15 keV) for improved sensitivity in the higher end (~26 to 48 keV range). The use of a monochromatic beam, which tends to be the standard mode of operation for most SR-XRF analyses reported in the literature, gave the least sensitive analysis.

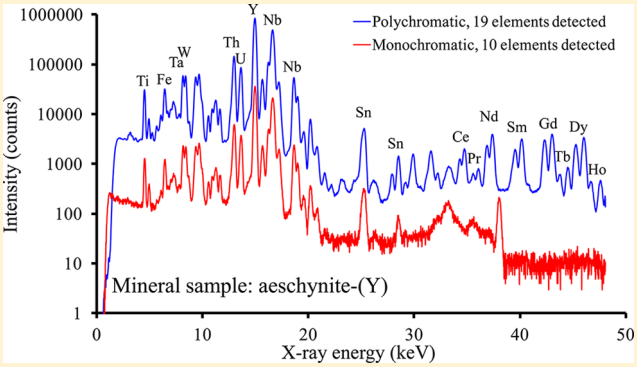

The trace elemental analysis of materials by X-ray methodologies, such as X-ray fluorescence (XRF), is a widespread and mature field.[1,2] The XRF methods have three primary advantages. The first advantage is that the analysis is nondestructive so it can be applied to historical or rare artifacts that cannot be damaged.[3−9] The second main advantage of the XRF methods is that they can be conducted at microscopic scales, termed μ-XRF, to map the elemental composition of a sample with a spatial resolution of 10 μm or less.[10−17] Lastly, XRF methods can be applied directly to samples which has resulted in a number of commercially available "portable" XRF units that can be used to determine elemental composition of samples in the field (for example, see refs 18 and 19). The main limitations of XRF methods are that they typically lack the sensitivity of inductively coupled plasma mass spectrometry (ICP-MS) and "thick" samples have X-ray self-absorption problems that make quantification more difficult.

The use of synchrotron radiation XRF (SR-XRF) has increased dramatically in recent years[20−23] as a means to conduct highly sensitive elemental analyses, some important aspects of which have been recently reviewed in the literature.[24] The SR-XRF uses an intense, polarized X-ray beam that, with proper location of the detector in the plane of polarization, lowers the background in the spectra by 1 order of magnitude or more, hence improving the sensitivity of the analysis. The relatively recent advances in X-ray detectors, namely the silicon drift detectors (SDD), provide considerably higher X-ray counting rates so these detectors are natural companions to the synchrotron excitation that can provide a high degree of sample excitation. The intensity of the beam can generate enough emissions from even small samples, as in micromapping experiments, to provide elemental spectra.

Many research groups around the world use SR-XRF for various trace element analyses, yet a discussion on the optimal conditions for different types of analyses is largely lacking in the literature. Most research groups simply use the synchrotron beamlines that are available to them because the beamlines are large, multiuser research facilities that are not amenable to major modification by individual research groups for specific studies. The majority[4−12,15−17,25,26] of trace element analyses take the polychromatic output from the synchrotron and pass it through a monochromator to generate a single, tunable excitation energy. The selection of a single energy for excitation provides the greatest selectivity for the analysis, but it comes at a cost of greatly reduced photon intensity that limits sample excitation. Another configuration is to utilize the total polarized polychromatic source beam from the synchrotron, which is

Received: May 5, 2014
Accepted: July 15, 2014

   dx.doi.org/10.1021/ac5016535 | *Anal. Chem.* XXXX, XXX, XXX−XXX

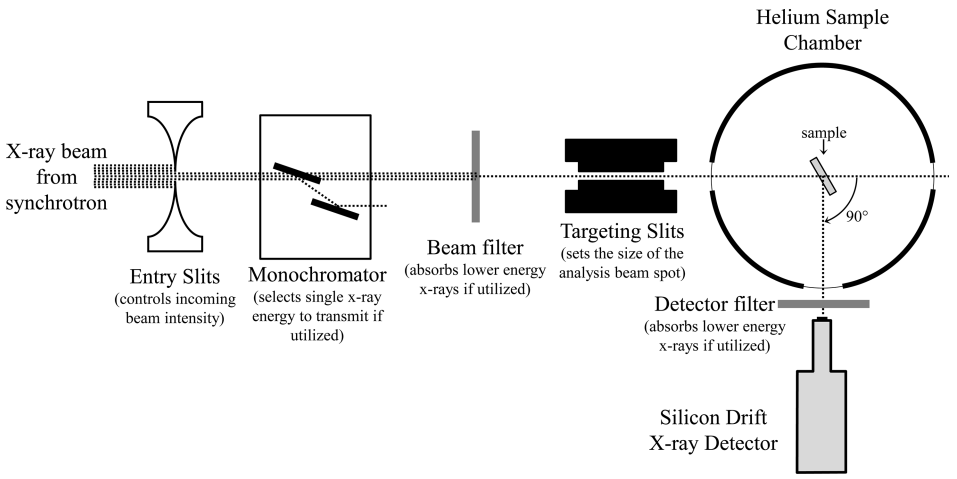

Figure 1. Schematic diagram of the components of SSRL beamline 2-2 utilized during this study.

often termed a "white beam", to excite the sample. This provides the least selective excitation mode but it has the greatest photon flux that may be needed to excite small amounts of sample mass.

Very few research groups use "white beam" synchrotron radiation for sample excitation. The only two groups we could locate were aerosol researchers based in California (using the Advanced Light Source beamline 10.3.1 in Berkeley)[27−30] and Switzerland (using both the Swiss Light Source and HASYLAB in Hamburg, Germany)[31−35] that employ similar methodologies. Both these groups were driven to "white beam" analyses by the small mass delivered by their use of time-resolved and size-segregated aerosol samplers. A potential intermediate option would be to use a primary beam filter to remove part of the polychromatic excitation energy in the region where maximum sensitivity is desired, thus lowering the background for a particular energy range of elements. The use of a primary beam filter (for example, see refs 1, 36, and 37) to increase sensitivity for selected elements is a widespread technique used by X-ray tube-based systems since the 1960s,[38] but it has been rarely utilized, or rarely reported, by the synchrotron research groups conducting elemental analyses.[31,34]

The objective of this study was to evaluate the performance of four different synchrotron beamline configurations for the elemental analysis of three typical environmental samples. The beamline configurations were all options that are typically available to users with minimal or no beamline modifications. The beamline configurations investigated were (1) a "white beam", which was the total, polychromatic X-ray emissions from the synchrotron, (2) a filtered white beam, (3) a filtered white beam and a filtered detector, and (4) a monochromatic X-ray beam generated by a Si(400) crystal. These beamline configurations were tested on a set of three typical environmental samples to determine which configuration was optimal for each type of sample. The environmental samples were chosen to represent different thicknesses of sample substrates typically analyzed by XRF. The samples selected for this evaluation study were a thin aerosol sample, an intermediate thickness biological sample, and a thick rare earth mineral specimen.

EXPERIMENTAL SECTION

The optimization of SR-XRF was conducted at the Stanford Synchrotron Radiation Lightsource (SSRL) at the SLAC National Accelerator Laboratory (SLAC). This instrument is a 3 GeV synchrotron that typically operates at a current of 450 to 500 mA. Beamline 2-2 was chosen for this study because it has widest range of X-ray energies and highest maximum energy of the beamlines at SSRL. The wide range of beam energies gives this beamline the greatest flexibility for optimization with beam filtering. The high maximum energy allows more elements to be detected using K lines, which is particularly advantageous for elements, such as Cd, Sb, and I, whose L-lines fall in the crowded, lower energy part of the spectrum. This beamline is also one of only two polychromatic-ready beamlines at the facility. The median X-ray energy for this beamline was approximately 20 keV, and the majority of the photon flux is below 40 keV. However, some photon flux was present at energies as high as 55 keV.

The experimental platform inside the hutch consisted of several components as shown in Figure 1 to control and modify the X-ray beam from the synchrotron. Prior to entering the hutch, the beam was passed through a set of entry slits that decreased the intensity of the beam delivered to the hutch. The maximum beam intensity was obtained when these slits were fully open. The incoming beam intensity was often decreased at this point to avoid excessive sample excitation that might saturate the X-ray detector.

The next beam control device (if utilized) was a monochromator that can transmit a single photon energy down the beamline. This monochromator employed a Si(400) crystal with a lattice spacing (or *d*-space) of 1.357755 Å that tends to perform well with higher energy X-rays. For this study, the monochromator was set to 38 keV so that maximum sensitivity would be achieved for elements with X-ray energies between 15 and 28 keV (or about Zr to Te, Th, and U). Additionally, the 38 keV beam energy resulted in the incoherent Compton peak falling in the relatively unimportant part of the spectrum near the $K_{\alpha 1}$ line of xenon. Because the monochromator transmits only a single X-ray energy from all of the energies available in the incident beam, the intensity of the transmitted beam was greatly decreased so the entry slits were typically completely open to deliver the maximum X-ray intensity.

dx.doi.org/10.1021/ac5016535 | *Anal. Chem.* XXXX, XXX, XXX−XXX

The next beam control device (if utilized) was a beam filter, the composition and thickness of which were optimized during this study. The beam filter absorbed a large fraction of the lower energy X-rays from the incoming X-ray beam while transmitting most of the higher energy X-rays. This resulted in an excitation beam with a greater proportion of the higher energy X-rays. It also lowered the background caused by Compton scattering in the part of the spectrum where the energy was absorbed. The beam filter decreases the intensity of the transmitted X-ray beam, but the decrease in beam intensity was not as large as from the monochromator. Four different metal foils (aluminum, zinc, molybdenum, and silver) and six different thicknesses of aluminum filters were tested as beam filters (Table 1 and Figure 2, respectively). The beam filter was optimized to increase the sensitivity for elements with K line X-ray energies between 20 and 48 keV, which includes many rare earth elements and the toxic elements of Cd, Sb, and Ba that are otherwise difficult to quantify using L line emissions in complex environmental samples with abundant light elements. Ultimately, a 4.1 mm thick aluminum filter was selected as the optimal filter for this beamline and application. The principle of filtering polychromatic X-ray sources to provide improved sensitivity for certain parts of the spectra is well established[1,36−38] and is used by some commercially available benchtop XRF systems. However, it is very rarely reported for SR-XRF analyses[31,34] and never discussed in great detail. The beam filter was never used in conjunction with the monochromator; the beam filter and monochromator represent two different ways to modify the incoming X-ray beam.

Table 1. Performance of Different SR-XRF Beam Filter Materials for Detecting Elements in a Rare Earth Mineral Sample, Aeschynite-(Y)[a]

	beam filter material			
	aluminum	zinc	molybdenum	silver[b]
beam filter thickness (mm)	4.1	0.62	0.25	0.50
beam filter areal density (g/cm^2)	1.1	0.44	0.32	0.36
total spectrum counts	2.8×10^7	2.1×10^7	1.8×10^7	5.7×10^6
Y ($K_{\alpha 1}$)	**1500**	840	1400	200
Th ($L_{\beta 1}$)	**460**[c]	280[c]	210[c]	70[c]
Nb ($K_{\alpha 1}$)	**2800**	1600	1800	410
U ($L_{\beta 1}$)	**340**[c]	210[c]	460[c]	100[c]
Ag ($K_{\alpha 1}$)	7.2	11	**12**	source[d]
Sn ($K_{\alpha 1}$)[e]	**330**	220	180	62
Sb ($K_{\alpha 1}$)	**7.7**	6.5	5.7	3.1
Ba ($K_{\alpha 1}$)	15	**18**	14	2.3
La ($K_{\alpha 1}$)	17	**17**	16	3.0
Ce ($K_{\alpha 1}$)	130	**180**	140	37
Pr ($K_{\alpha 1}$)	30	**46**	33	9.8
Nd ($K_{\alpha 1}$)	260	**420**	330	110
Sm ($K_{\alpha 1}$)	180	**340**	280	110
Gd ($K_{\alpha 1}$)	200	**430**	370	200
Tb ($K_{\alpha 1}$)	33	**72**	57	40
Dy ($K_{\alpha 1}$)	170	**370**	350	240
Ho ($K_{\alpha 1}$)	18	**43**	40	33

[a]The aluminum filter acted as a simple mass filter while the other three element filters used an absorption edge to lower the excitation X-ray background for specific energies in the range between 10 and 25 keV. The values represented in the table are the signal-to-noise ratios for the elements detected. The elements are listed in increasing order of their X-ray energies and the particular X-ray emission line used for the sensitivity assessment is given in parentheses. All tests were conducted with a detector filter consisting of 2 mm of aluminum, which removed the lower part of the spectrum. The best beam filter for a particular element is shown in bold text. [b]The silver foil reduced the intensity of the excitation beam to the point where the detector could not operate at an effective count rate. [c]The peak measured may consist of overlapping X-ray emissions from two elements. This also includes peaks that are on the shoulder of another peak. [d]The emission of silver X-rays from the sample could not be quantified because there may be additional silver X-rays from the fluorescence of the beam filter. The amount of fluorescence X-rays from the beam filter was remarkably small (and not even detected for the molybdenum filter). [e]The tin peak was also observed in blank spectra, so it may be the result of the detector or other nearby materials.

If neither the monochromator nor the beam filter was utilized, then a "white beam" was transmitted down the beamline. This was simply the full spectrum (i.e., polychromatic spectrum) of X-rays generated by the synchrotron, nominally 4 to 40 keV. The white beam had the greatest transmitted flux, but it was the least selective in terms of X-ray energies transmitted.

The next stage of the beamline was the beam control slits that control the size of the beam spot (or sampling area). For this study, the beam spot was 1.0 × 0.5 mm unless otherwise noted, but this value can be set from anywhere between about 0.5 × 0.5 mm to 6 × 2 mm. Larger beam spots sample more area (and sample mass) and thus generate more X-ray emissions. Smaller spots are preferred for samples with spatial heterogeneity, but it comes at a cost of lower X-ray flux passing through the sample and hence fewer X-ray emissions from the sample.

The transmitted X-ray beam passes into a helium chamber where the samples are mounted. The helium atmosphere between the samples and the X-ray detector allows for the detection of low-energy X-rays that would otherwise be absorbed by the air. The helium chamber was simply a vertically mounted acrylic cylinder that is almost completely sealed except for a small hole on the bottom that allows for sample insertion. Windows were cut into the chamber for the entry and exit of the X-ray beam as well as for the detector. The windows were covered with a very thin layer of Kapton (DuPont) to keep the helium in the chamber but allow X-ray transmission with effectively no attenuation at the X-ray energies being used in this study. The chamber has a steady stream of helium (0.03 m^3 per hour) going through it with any extra helium escaping from the hole on the bottom of the chamber where the samples were inserted.

The X-rays generated by the sample then may pass through a detector filter if it was utilized. Detector filters have been used in prior studies (e.g.,[26,39,40]) to suppress detection of abundant low-end elements. The composition and the thickness of the detector filter can be easily changed depending on the particular application to remove a particular range of the spectrum. In this study, the detector filter consisted of 2.0 mm of aluminum to absorb lower energy X-rays (below about 15 keV) before they reach the detector. This sacrifices the lower range of the spectrum to give improved sensitivity for elements with higher energy X-rays because the detector will not be overwhelmed by X-rays from common and abundant elements like iron[39] and calcium.[26]

The last part of the beamline was the SII Vortex EX X-ray detector (Hitachi High-Technologies Science America, Inc.)[41]

dx.doi.org/10.1021/ac5016535 | Anal. Chem. XXXX, XXX, XXX−XXX

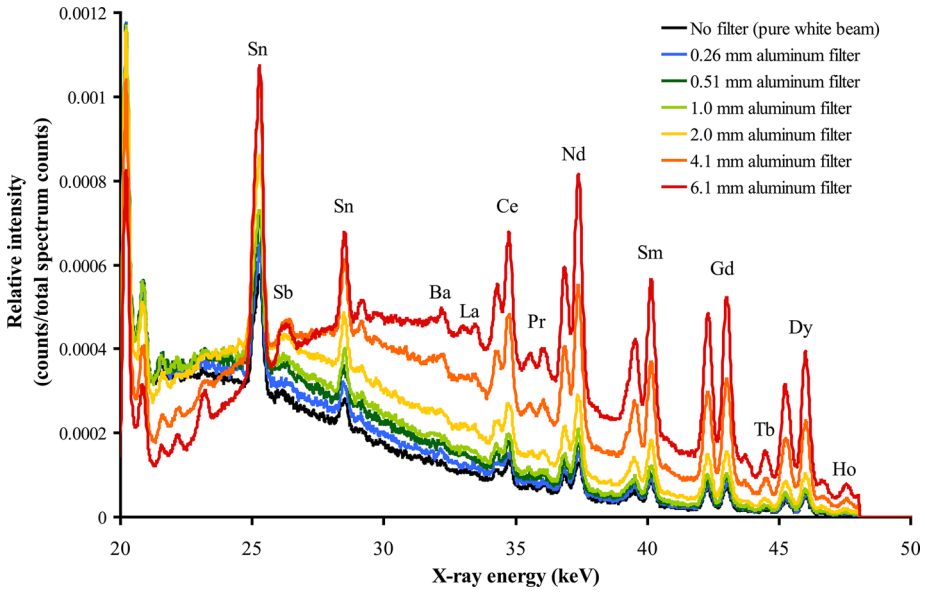

Figure 2. Optimization of the thickness of the aluminum beam filter for the analysis of rare earth elements in a mineral sample of aeschynite-(Y). These analyses were conducted using a 2 mm aluminum detector filter to suppress the low-energy part of the spectrum. Both the 4.1 mm and 6.1 mm aluminum beam filters allowed the detection of more elements than thinner beam filters. However, the 6.1 mm filter reduced the beam intensity too much for the analysis of thinner samples, so the 4.1 mm filter thickness was chosen as the optimal thickness for the range of samples investigated in this study. The 4.1 mm aluminum filter was made by folding a sheet of regular Reynolds Wrap aluminum foil (98.5% pure aluminum with iron and silicon making up the remaining 1.5%) eight times to give 256 layers of aluminum foil.

that quantified the number and the energy of the X-rays emitted from the sample. This was a silicon drift detector that can process the higher count rates found in synchrotron applications. In this study, the detector was operated at an optimal count rate that resulted in a detector dead-time of approximately 20%. The entry slits were adjusted to deliver a beam intensity to keep the detector operating at the optimal count rate. If the entry slits were completely open and the detector was still below the optimal count rate, then it was noted in the results that maximum performance could not be obtained. The detector was mounted at 90° relative to the X-ray beam to take maximum advantage of the polarized nature of the X-ray beam. However, this detector angle makes it more likely that diffraction peaks may appear in the spectra of crystalline mineral samples when using polychromatic excitation methods.

Three environmental samples were chosen to represent different matrixes that are typically analyzed by X-ray fluorescence. The first sample was a particulate air sample collected on a mylar impaction substrate with an eight-stage DRUM sampler[42] downwind of the railroad repair depot in Roseville, CA.[43] The particulate size fraction represented by this sample was the 0.09 to 0.26 μm size fraction. This sample represents a very thin sample with an areal density of 132 μg/cm^2 on a mylar substrate with a density of 480 μg/cm^2. This thin sample is unlikely to experience any significant X-ray self-absorption or incoming excitation beam attenuation. The second environmental sample was a biological sample, namely the keratin rattle from a sidewinder rattlesnake (*Crotalus cerastes*). The sample was collected in a relatively rural area south of Phoenix, AZ. This sample has an "intermediate" thickness with an areal density of 47 mg/cm^2 that may result in some of the lower-energy X-rays (e.g., sulfur) being self-absorbed by the sample matrix; hence, some corrections need to be applied to obtain quantitative results. The excitation beam is unlikely to experience any appreciable attenuation passing through the sample. The last of the representative environmental samples chosen was a rare earth mineral sample, namely aeschynite-(Y) from Hittero, Norway, with a reported formula of (Y, Ca, Fe, Th)(Ti, Nb)$_2$(O, OH)$_6$. This sample was about 2 mm thick, but this is considered a "thick" target in terms of X-ray analysis, which means that many of the lighter elements (e.g., Ca and Ti) will be under-represented in the spectrum due to matrix self-absorption effects. Furthermore, the excitation beam is likely to experience significant attenuation penetrating the sample. While absolute quantification by the application of absorption corrections is possible, this type of analysis is best for qualitative or comparative results. The sample run time was 10 min for every analysis in this study.

RESULTS AND DISCUSSION

The four different beamline configurations were evaluated on (1) their ability to detect a wide range of elements (Figure 3), and (2) the sensitivity for the elements that were detected (Table 2). The four different configurations had strengths and weaknesses so the different configurations were optimal for different types of samples. The beamline configurations evaluated represented a trade-off between beam intensity and beam selectivity. One end of the continuum was the white beam that was very intense but not selective. The other end was represented by the monochromatic beam that was highly selective but had low intensity. The samples selected for evaluation were chosen to illustrate the benefits of the different parts of the intensity−selectivity continuum. The aerosol sample with a very low mass was expected to perform the best with a highly intense but nonselective white beam. The mineral sample was the opposite extreme where trace concentrations of rare earth elements were the focus in a mineral that was dominated by Ti, Y, and Nb; hence, the selective nature of the analysis was expected to be beneficial.

Overall, the white beam configuration provided good results over a wide range of elements in that it was able to detect 11

dx.doi.org/10.1021/ac5016535 | *Anal. Chem.* XXXX, XXX, XXX−XXX

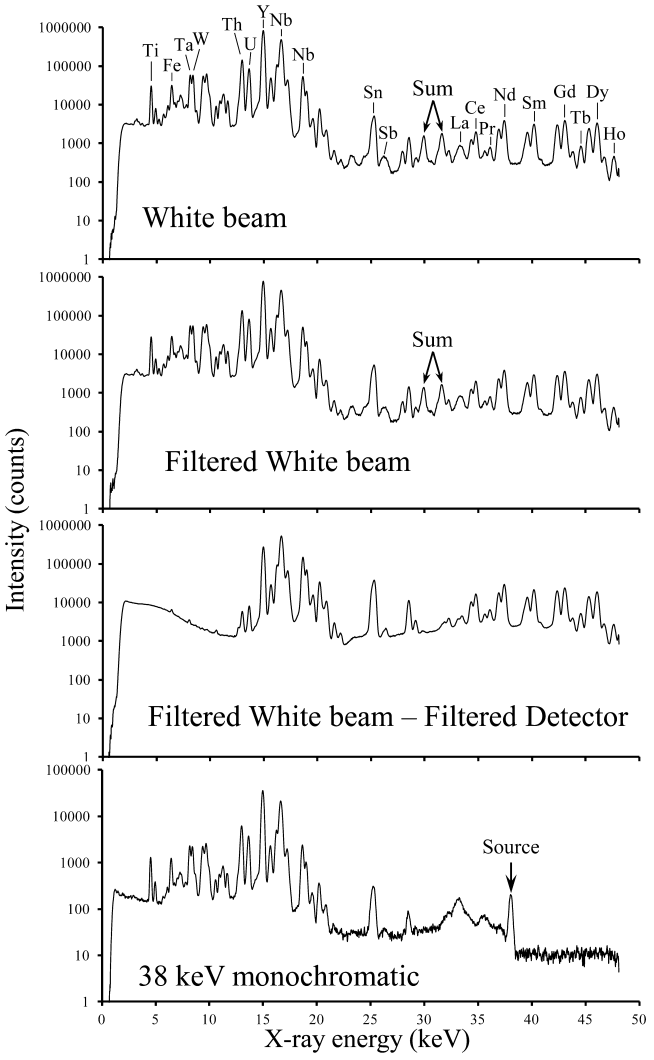

Figure 3. Spectra obtained from a sample of the rare earth mineral aeschynite-(Y) with the four beamline configurations investigated. Notice that the filtered white beam–filtered detector configuration cannot obtain the low end of the spectrum while the monochromatic beam cannot obtain the high end of the spectrum. The two peaks labeled with "Sum" in the white beam and filtered white beam spectra are an artifact called "sum peaks" along with a few smaller peaks in that area of the spectrum. Notice that the sum peaks are absent from the filtered white beam–filtered detector and the monochromatic spectra.

elements in the aerosol sample, 21 in the rattlesnake tail, and 19 in the mineral specimen (Table 2). Moreover, there were no elements that were expressly excluded by this analysis. Elements from potassium to holmium could be detected with the K line X-rays, and elements from erbium to uranium could be detected with the L line X-rays. The sensitivity of the analysis, as measured by the signal-to-noise ratios, was frequently better than the other configurations with the white beam being the most sensitive in 8 of the 15 elements detected in the aerosol sample and 11 of 22 elements detected in the rattlesnake tail. Surprisingly, the white beam was the best for only one element in the mineral sample. The white beam tended to be the best for elements with lower energy X-rays (e.g., 12 keV or lower) because the white beam has more low-energy X-rays to excite these elements. The white beam analyses are particularly effective for samples with very low masses, such as aerosol samples or microprobe analyses that require a high photon flux to generate enough emissions for a sensitive spectrum. It is worth noting that the only two research groups we could find that utilized white beam analyses were primarily conducting aerosol analysis where amounts of material analyzed are very small.[29,31]

The limitations of the white beam were relatively few. In thick samples, the white beam system tended to have high count rates from common elements (e.g., iron) that limited the sensitivity for rarer elements (e.g., antimony). Furthermore, the presence of intense emission lines from abundant elements increases the occurrence of sum peaks in the spectra (Figure 3), which are the result of two low-energy X-rays from an abundant element hitting the detector at the exact same time and appearing as a fictitious peak equal to the sum of their energies. In the rare earth mineral sample, a sum peak was observed in the white beam and filtered white beam analyses corresponding to the sum of two Y K_α X-rays, but the sum peak was relatively minor at 0.13% of the intensity of the Y K_α peak. Sum peaks can also be reduced by lowering beam intensity so that the detector operates at a lower count rate (i.e., detector dead-time is reduced).

The other limitation of the white beam configuration was that it was vulnerable to diffraction peaks in crystalline mineral samples. Diffraction peaks occur when one of the many wavelengths of incoming source X-ray matches a wavelength that can diffract off of a crystalline material. This causes a coherent beam of source X-rays at a particular energy to strike the detector, which gives a peak in the energy spectrum. These diffraction peaks can complicate the data interpretation because they can masquerade as elemental emission peaks. While no diffraction peaks were observed in the samples analyzed in this experiment, they have been observed in other mineral samples analyzed by our group with the white beam. Diffraction peaks can be reduced or eliminated by powdering crystalline samples and using a larger beam spot to integrate over a larger area.

The filtered white beam performed better than the white beam for elements with X-ray energies between 11 and 26 keV, which roughly corresponds to bromine to antimony. In the aerosol sample, the filtered white beam performed best for 7 of the 15 elements detected. Furthermore, it was able to detect an additional 4 elements (Sr, Mo, Ag, and Sb) that were not detected by the other beamline configurations. For the rattlesnake tail, the filtered white beam was the most sensitive for 9 elements of the 22 elements detected. The filtered white beam also performed well on the mineral sample (11 out of 23 elements detected). The filtered white beam detected more elements in the three environmental samples than any other beamline configuration. The increased sensitivity to the higher energy elements was accomplished by two processes: (1) increasing the proportion of higher energy X-rays in the incoming beam by absorbing the lower energy photons and (2) lowering the background of Compton X-rays in regions of the spectra with elements of interest. The filtered white beam configuration also performed the best with thicker samples (e.g., biological and mineral specimens).

The filtered white beam–filtered detector configuration was designed to increase the sensitivity of the system for the elements with the highest X-ray energies by placing a filter over the detector to eliminate the lower energy X-rays from abundant elements like calcium and iron.[26,39] This means all of the X-rays counted by the detector originate from the higher end of the energy spectrum. However, the addition of the detector filter forsakes the lower end of the spectrum with its

dx.doi.org/10.1021/ac5016535 | Anal. Chem. XXXX, XXX, XXX–XXX

Table 2. Performance of the Different Beamline Configurations for Detecting Elements in the Three Representative Sample Types[a]

	thin aerosol sample (Roseville, CA)			intermediate biological sample (rattlesnake tail, Phoenix, AZ)				thick mineral sample (Aeschynite-(Y), Hittero, Norway)			
	WB	FWB	Mono	WB	FWB	FWB-FD	Mono	WB	FWB	FWB-FD	Mono
no. of detections	11	15	4	21	22	10	9	19	23	17	10
counts	3.5×10^7	1.9×10^7	9.5×10^4	5.2×10^7	4.0×10^7	1.1×10^7	7.4×10^5	3.3×10^7	3.1×10^7	2.8×10^7	1.4×10^6
K ($K_{\alpha 1}$)	INT	INT	ND	**240**	170	–	ND	ND	ND	–	ND
Ca ($K_{\alpha 1}$)	**59**	4.5	ND	**1700**	1300	–	1.2	2.3	**2.8**	–	ND
Ti ($K_{\alpha 1}$)	**200**	14	INT	**470**	430	–	8.8	160	**190**	–	31
V ($K_{\alpha 1}$)	INT	ND	ND	**90**[b]	83[b]	–	INT	26[b]	**32**[b]	–	INT
Cr ($K_{\alpha 1}$)	**25**	4.2	ND	**32**	11	–	ND	ND	ND	–	ND
Mn ($K_{\alpha 1}$)	**20**	1.9	ND	**590**	460	–	ND	ND	ND	–	ND
Fe ($K_{\alpha 1}$)	**1400**	150	2.1	**22000**	17000	–	34	140	**180**	–	29
Ni ($K_{\alpha 1}$)	**130**	13	ND	62	**73**	–	ND	ND	INT	–	INT
Cu ($K_{\alpha 1}$)	**180**	33	2.6	**280**	270	–	1.8	INT	INT	–	INT
Ta ($L_{\alpha 1}$)	INT	INT	ND	INT	INT	–	ND	ND	**360**	–	55
W ($L_{\alpha 1}$)	ND	ND	ND	ND	ND	–	ND	ND	**370**	–	56
Zn (K_{α})	**320**	30	9.1	**710**	550	–	7.8	INT	ND	–	ND
Se ($K_{\alpha 1}$)	ND	ND	ND	**4.6**	4.0	–	ND	INT	INT	–	INT
Br ($K_{\alpha 1}$)	19	**28**	ND	**110**	100	–	0.8	ND	ND	–	ND
Pb ($L_{\beta 1}$)	17	**47**	ND	21[b]	**75**[b]	–	ND	32[b]	**62**[b]	–	10
Rb ($K_{\alpha 1}$)	ND	ND	ND	120	**120**	3.7	ND	INT	INT	ND	ND
Sr ($K_{\alpha 1}$)	ND	**11**	ND	360	**440**	32	2.6	ND	ND	ND	ND
Y ($K_{\alpha 1}$)	ND	ND	ND	38[b]	**50**[b]	8.9[b]	ND	6000	**8900**	1500	990
Zr ($K_{\alpha 1}$)	ND	ND	ND	110[b]	**160**[b]	47[b]	1.9	INT	INT	INT	INT
Th ($L_{\beta 1}$)	ND	ND	ND	ND	ND	ND	ND	300	**1000**[b]	460[b]	120
Nb ($K_{\alpha 1}$)	ND	ND	ND	6.5	**15**	6.9	ND	3200	**4900**	2800	570
U ($L_{\beta 1}$)	ND	ND	ND	ND	ND	ND	ND	300[b]	**470**[b]	340[b]	51
Mo ($K_{\alpha 1}$)	ND	**7.0**	ND	ND	ND	ND	ND	INT	INT	INT	ND
Pd ($K_{\alpha 1}$)	ND	ND	ND	ND	ND	1.0	ND	ND	ND	ND	ND
Ag ($K_{\alpha 1}$)	ND	**5.8**	ND	10	**13**	13	ND	**13**	0.8	7.2	ND
Sn ($K_{\alpha 1}$)[c]	17	**130**	4.0	14	**38**	35	1.8	300	88	**330**	14
Sb ($K_{\alpha 1}$)	ND	**7.1**	ND	ND	2.2	**2.3**	ND	ND	ND	**7.7**	ND
Ba ($K_{\alpha 1}$)	ND	ND	ND	3.8	9.7	**18**	ND	8.7	5.6	**15**	ND
La ($K_{\alpha 1}$)	ND	ND	–	ND	ND	ND	–	17	8.4	**17**	–
Ce ($K_{\alpha 1}$)	ND	ND	–	ND	ND	ND	–	49	33	**130**	–
Pr ($K_{\alpha 1}$)	ND	ND	–	ND	ND	ND	–	13	7.3	**30**	–
Nd ($K_{\alpha 1}$)	ND	ND	–	ND	ND	ND	–	110	76	**260**	–
Sm ($K_{\alpha 1}$)	ND	ND	–	ND	ND	ND	–	86	56	**180**	–
Gd ($K_{\alpha 1}$)	ND	ND	–	ND	ND	ND	–	110	70	**200**	–
Tb ($K_{\alpha 1}$)	ND	ND	–	ND	ND	ND	–	9.7	10	**33**	–
Dy ($K_{\alpha 1}$)	ND	ND	–	ND	ND	ND	–	95	55	**170**	–
Ho ($K_{\alpha 1}$)	ND	ND	–	ND	ND	ND	–	11	6.5	**18**	–

[a]The values represented in the table are the signal-to-noise ratios for the elements detected rounded to two significant digits of accuracy. If an element was outside the range of elements that could be detected by a configuration, then it is denoted as "–". If an element was within the range of elements that could be detected by a configuration but it was not observed, then it is denoted as "ND" if the baseline was relatively flat or "INT" if there was a large, interfering peak that would obscure the element. The elements are listed in increasing order of their X-ray energies, and the particular X-ray emission line used for the sensitivity assessment is given in parentheses. The beamline configurations are abbreviated as follows: "WB" is white beam, "FWB" is filtered white beam (using a 4.1 mm Al filter), "FWB-FD" is filtered white beam with filtered detector (using a 4.1 mm Al filter on the beam and a 2 mm Al filter on the detector), and "Mono" is monochromatic beam. The most sensitive configuration for each element in each of the test samples is highlighted in bold text. [b]The peak measured may consist of overlapping X-ray emissions from two elements. This also includes peaks that are on the shoulder of another peak. [c]The tin peak was also observed in blank spectra, so it may be the result of the detector or other nearby materials.

many interesting and toxic elements. The filtered white beam–filtered detector performed poorly for the aerosol and rattlesnake samples that were dominated by elements in the lower end of the spectrum. The aerosol sample was unable to achieve anywhere near optimal detector count rate even at maximum synchrotron beam intensity; hence, the data was not collected. For the rattlesnake tail, this configuration was the best for a single element, namely barium, out of the 22 elements detected. However, the filtered white beam–filtered detector was very effective at analyzing the rare earth mineral specimen because this configuration was the most sensitive for 12 elements with X-ray energies between 26 and 47 keV (or about antimony to holmium). Unfortunately, the configuration used in this study effectively sacrifices all elements with X-ray energies below about 15 keV, which encompasses most of the common elements normally detected by XRF. One fringe benefit of excluding the abundant low-energy elemental emissions is that it dramatically reduces the presence of "sum

dx.doi.org/10.1021/ac5016535 | Anal. Chem. XXXX, XXX, XXX–XXX

peaks" higher in the spectrum that might interfere with the detection of trace amounts of elements (Figure 3). Overall, the filtered beam-filtered detector was a more specialized configuration for the analysis of more energetic elements.

The monochromatic beam performed poorly compared to the other beam configurations. Simply, the lower photon flux resulting from transmitting a single frequency of light was not able to generate enough X-rays from the samples to operate the detector at efficient count rate. The beam spot size in the monochromatic analyses was even increased to 6 mm × 2 mm, compared to the 1 mm × 0.5 mm of the other analyses, to compensate for the lower photon flux. Even under these large beam spot conditions, the monochromatic beam was always the least sensitive configuration in terms of both signal-to-noise and the number of elements detected. Furthermore, the monochromatic beam at 38 keV was unable to excite elements with higher X-ray energies, such as the K lines of the rare earth elements. The monochromatic beam at 38 keV was especially insensitive to the elements with low X-ray energies (<8 keV) because the absorption cross-section of these elements was low. The monochromatic beam was best suited for mineral samples where the large mass of the sample can partly offset the effect of a low photon flux, but the other beamline configurations provided considerably greater sensitivity. One inherent advantage of the monochromatic beam was that it was effectively immune to diffraction peak artifacts in the spectrum when analyzing crystalline samples.

Ultimately, the X-ray detector represented the limiting factor in most SR-XRF analyses because the detector had a finite count rate. The synchrotron beams were generally able to provide greater sample excitation than the detector can process, so the optimization of the beamline was designed to adjust the X-rays reaching the detector to provide the greatest sensitivity in a particular part of the spectrum of interest to the analyst. The white beam was the best for a general analysis over a broad range of elements while the filtered configurations gave improved sensitivity in the more energetic parts of the spectrum at the expense of the lower energy elements.

The purpose of this research was to illustrate simple methods to enhance the sensitivity of SR-XRF analyses. Almost all of the SR-XRF studies use a monochromator, yet the results show that a monochromatic source was less sensitive than other options due to the dramatic decrease in photon flux that limited the amount of sample excitation. Monochromators are essential to other synchrotron applications, such as X-ray crystallography, X-ray absorption near-edge structure (XANES), etc.; hence, monochromators are common on synchrotron beamlines and are probably used mainly by default. This study was conducted to evaluate alternatives to a monochromator by filtering the source X-ray beam or detector to achieve increased sensitivity in selected energy ranges in the spectrum.

The results of this study indicate that dramatic increases in sensitivity can be achieved by SR-XRF by simply removing the monochromator and using a white beam. The simplest way to achieve this is to remove the crystals from the monochromator and allow the white beam to pass unmodified through the monochromator housing. The use of a white beam increases sample excitation by orders of magnitude yet the polarized nature of the X-ray beam keeps the background relatively low. Bukowiecki et al.[31] also demonstrated that a white beam was far more sensitive than a monochromatic beam for thin aerosol analysis, yet almost all other research groups still use a monochromatic beam for SR-XRF.

The second option is to use a primary beam filter when using a white beam. The advantage of filters is that they are simply sheets of metal that can be placed in the beamline, so they do not require any significant modification to the synchrotron facility yet they deliver enhanced sensitivity for some elements. It is recommended to place the primary beam filter as far "upstream" in the beamline as possible so that any fluorescent emissions from the filter material will have spread out before they reach the sample or the detector.

The use of detector filters can dramatically increase the sensitivity of the analysis for select elements with higher energy X-rays at the expense of the elements with lower energy X-rays. Detector filters seem to be best suited for trace analysis of samples with considerable mass whose matrix is dominated by lighter elements such as calcium, iron, and zinc. One advantage of detector filtering is that multiple detectors can be deployed around the sample with different degrees of detector filtering. This allows one unfiltered detector to obtain the full spectrum of elements while a second (or even third) detector may be filtered to give greater sensitivity for the elements with more energetic X-rays. Given the limitations on synchrotron beam time, a multiple detector array with some detectors filtered could provide the greatest sensitivity over a wide range of elements for the least amount of beam time. Another potential option is to employ a pierced filter, also sometimes called a "funny filter",[40] that has a small hole drilled in it to allow a small fraction of the low-energy X-ray to reach the detector unimpeded while blocking the rest. This suppresses the intensity of abundant low-energy elements while still obtaining a complete spectrum.

■ CONCLUSIONS

The vast majority of SR-XRF studies reported in the literature utilize a monochromatic beam for sample excitation. However, the results from this study and a prior one by Bukowiecki et al.[31] indicate that dramatic increases in sensitivity can be obtained by simply removing the monochromator and using the polychromatic white beam from the synchrotron for sample excitation. This is especially true when using the fast X-ray detectors such as the silicon drift detectors. The advantage of this approach is that no new equipment is needed and the modifications, which generally consist of removing the crystals from the monochromator housing, are simple. Both primary white beam filters and detector filters represent ways to easily customize the analysis to focus on different parts of the energy spectrum. A multiple detector array, where one or more of the detectors are filtered, could provide the greatest sensitivity over a wide range of elements in the least amount of synchrotron beam time. The filtering methods used in this study have been used by X-ray tube XRF operators for decades, yet they have not been widely adopted by the SR-XRF researchers even though they could increase the sensitivity or selectivity of the analysis.

■ AUTHOR INFORMATION

Corresponding Author

*E-mail: tmcahill@asu.edu.

Notes

The authors declare no competing financial interest.

dx.doi.org/10.1021/ac5016535 | Anal. Chem. XXXX, XXX, XXX−XXX

■ ACKNOWLEDGMENTS

Portions of this research were carried out at the Stanford Synchrotron Radiation Lightsource, a Directorate of SLAC National Accelerator Laboratory and an Office of Science User Facility operated for the U.S. Department of Energy Office of Science by Stanford University. We thank the wonderful staff at SSRL who made this research project possible. In particular, we thank Tom Hostetler and David Day for their help setting up the beamline. This project was supported in part through a Cooperative Agreement with the Army Research Laboratory (W911NF-12-2-0068) and the University of Alaska, Fairbanks.

■ REFERENCES

(1) Margui, E.; Van Grieken, R. *X-Ray Fluorescence Spectrometry and Related Techniques*; Momentum Press: New York, 2013.
(2) Tsuji, K.; Nakano, K.; Takahashi, Y.; Hayashi, K.; Ro, C.-U. *Anal. Chem.* **2012**, *84*, 636−668.
(3) Bertrand, L.; Cotte, M.; Stampanoni, M.; Thoury, M.; Marone, F.; Schoeder, S. *Phys. Rep.* **2012**, *519*, 51−96.
(4) Geil, E. C.; LeBlanc, S. A.; Dale, D. S.; Thorne, R. E. *J. Archaeol. Sci.* **2013**, *40*, 4780−4784.
(5) Manning, P. L.; Edwards, N. P.; Wogelius, R. A.; Bergmann, U.; Barden, H. E.; Larson, P. L.; Schwarz-Wings, D.; Egerton, V. M.; Sokaras, D.; Mori, R. A.; Sellers, W. I. *J. Anal. At. Spectrom.* **2013**, *28*, 1024−1030.
(6) Van der Snickt, G.; Janssens, K.; Dik, J.; De Nolf, W.; Vanmeert, F.; Jaroszewicz, J.; Cotte, M.; Falkenberg, G.; Van der Loeff, L. *Anal. Chem.* **2012**, *84*, 10221−10228.
(7) Dik, J.; Janssens, K.; Van der Snickt, G.; van der Loeff, L.; Rickers, K.; Cotte, M. *Anal. Chem.* **2008**, *80*, 6436−6442.
(8) Monico, L.; Van der Snickt, G.; Janssens, K.; De Nolf, W.; Miliani, C.; Dik, J.; Radepont, M.; Hendriks, E.; Geldof, M.; Cotte, M. *Anal. Chem.* **2011**, *83*, 1224−1231.
(9) Constantinescu, B.; Vasilescu, A.; Radtke, M.; Reinholz, U. *J. Anal. At. Spectrom.* **2011**, *26*, 917−921.
(10) Howard, D. L.; de Jonge, M. D.; Lau, D.; Hay, D.; Varcoe-Cocks, M.; Ryan, C. G.; Kirkham, R.; Moorhead, G.; Paterson, D.; Thurrowgood, D. *Anal. Chem.* **2012**, *84*, 3278−3286.
(11) Donner, E.; Howard, D. L.; de Jonge, M. D.; Paterson, D.; Cheah, M. H.; Naidu, R.; Lombi, E. *Environ. Sci. Technol.* **2011**, *45*, 7249−7257.
(12) Zimmer, D.; Kruse, J.; Baum, C.; Borca, C.; Laue, M.; Hause, G.; Meissner, R.; Leinweber, P. *Sci. Total Environ.* **2011**, *409*, 4094−4100.
(13) Evens, R.; De Schamphelaere, K. A. C.; De Samber, B.; Silversmit, G.; Schoonjans, T.; Vekemans, B.; Balcaen, L.; Vanhaecke, F.; Szaloki, I.; Rickers, K.; Falkenberg, G.; Vincze, L.; Janssen, C. R. *Environ. Sci. Technol.* **2012**, *46*, 1178−1184.
(14) Majumdar, S.; Peralta-Videa, J. R.; Castillo-Michel, H.; Hong, J.; Rico, C. M.; Gardea-Torresdey, J. L. *Anal. Chim. Acta* **2012**, *755*, 1−16.
(15) Manceau, A.; Nagy, K. L.; Marcus, M. A.; Lanson, M.; Geoffroy, N.; Jacquet, T.; Kirpichtchikova, T. *Environ. Sci. Technol.* **2008**, *42*, 1766−1772.
(16) Oakes, M.; Weber, R. J.; Lai, B.; Russell, A.; Ingall, E. D. *Atmos. Chem. Phys.* **2012**, *12*, 745−756.
(17) Waker, S. R.; Jamieson, H. E.; Rasmussen, P. E. *Environ. Sci. Technol.* **2011**, *45*, 8233−8240.
(18) Bardelli, F.; Barone, G.; Crupi, V.; Longo, F.; Majolino, D.; Mazzoleni, P.; Venuti, V. *Anal. Bioanal. Chem.* **2011**, *399*, 3147−3153.
(19) Potts, P. J.; West, M. *Portable X-ray Fluorescence Spectrometry: Capabilities for In Situ Analysis*; Royal Society of Chemistry: Cambridge, UK, 2008.
(20) West, M.; Ellis, A. T.; Potts, P. J.; Streli, C.; Vanhoof, C.; Wegrzynek, D.; Wobrauschek, P. *J. Anal. At. Spectrom.* **2010**, *25*, 1503−1545.
(21) West, M.; Ellis, A. T.; Potts, P. J.; Streli, C.; Vanhoof, C.; Wegrzynek, D.; Wobrauschek, P. *J. Anal. At. Spectrom.* **2011**, *26*, 1919−1963.
(22) West, M.; Ellis, A. T.; Potts, P. J.; Streli, C.; Vanhoof, C.; Wegrzynek, D.; Wobrauschek, P. *J. Anal. At. Spectrom.* **2012**, *27*, 1603−1644.
(23) West, M.; Ellis, A. T.; Potts, P. J.; Streli, C.; Vanhoof, C.; Wegrzynek, D.; Wobrauschek, P. *J. Anal. At. Spectrom.* **2013**, *28*, 1544−1590.
(24) Iida, A. *Encyclopedia of Analytical Chemistry*; Wiley: New York, 2013; pp 1−23
(25) Gherase, M. R.; Desouza, E. D.; Farquharson, M. J.; McNeill, F. E.; Kim, C.-Y.; Fleming, D. E. B. *Physiol. Meas.* **2013**, *34*, 1163−1177.
(26) Limburg, K. E.; Huang, R.; Bilderback, D. H. *X-Ray Spectrom.* **2007**, *36*, 336−342.
(27) Perry, K. D.; Cliff, S. S.; Jimenez-Cruz, M. P. *J. Geophys. Res.: Atmos.* **2004**, *109*, DOI: 10.1029/2004jd004979.
(28) VanCuren, R. A.; Cahill, T.; Burkhart, J.; Barnes, D.; Zhao, Y.; Perry, K.; Cliff, S.; McConnell, J. *Atmos. Environ.* **2012**, *52*, 82−97.
(29) Cahill, T. A.; Cliff, S. S.; Perry, K. D.; Jimenez-Cruz, M.; Bench, G.; Grant, P.; Ueda, D.; Shackelford, J. F.; Dunlap, M.; Meier, M.; Kelly, P. B.; Riddle, S.; Selco, J.; Leifer, R. *Aerosol Sci. Technol.* **2004**, *38*, 165−183.
(30) Bench, G.; Grant, P. G.; Ueda, D.; Cliff, S. S.; Perry, K. D.; Cahill, T. A. *Aerosol Sci. Technol.* **2002**, *36*, 642−651.
(31) Bukowiecki, N.; Lienemann, P.; Zwicky, C. N.; Furger, M.; Richard, A.; Falkenberg, G.; Rickers, K.; Grolimund, D.; Borca, C.; Hill, M.; Gehrig, R.; Baltensperger, U. *Spectrochim. Acta, Part B* **2008**, *63*, 929−938.
(32) Bukowiecki, N.; Lienemann, P.; Hill, M.; Furger, M.; Richard, A.; Amato, F.; Prevot, A. S. H.; Baltensperger, U.; Buchmann, B.; Gehrig, R. *Atmos. Environ.* **2010**, *44*, 2330−2340.
(33) Bukowiecki, N.; Lienemann, P.; Hill, M.; Figi, R.; Richard, A.; Furger, M.; Rickers, K.; Falkenberg, G.; Zhao, Y.; Cliff, S. S.; Prevot, A. S. H.; Baltensperger, U.; Buchmann, B.; Gehrig, R. *Environ. Sci. Technol.* **2009**, *43*, 8072−8078.
(34) Richard, A.; Bukowiecki, N.; Lienemann, P.; Furger, M.; Fierz, M.; Minguillon, M. C.; Weideli, B.; Figi, R.; Flechsig, U.; Appel, K.; Prevot, A. S. H.; Baltensperger, U. *Atmos. Meas. Tech.* **2010**, *3*, 1473−1485.
(35) Richard, A.; Gianini, M. F. D.; Mohr, C.; Furger, M.; Bukowiecki, N.; Minguillon, M. C.; Lienemann, P.; Flechsig, U.; Appel, K.; DeCarlo, P. F.; Heringa, M. F.; Chirico, R.; Baltensperger, U.; Prevot, A. S. H. *Atmos. Chem. Phys.* **2011**, *11*, 8945−8963.
(36) Ogawa, R.; Ochi, H.; Nishino, M.; Ichimaru, N.; Yamato, R. *X-Ray Spectrom.* **2010**, *39*, 399−406.
(37) Cossio, R.; Vaggelli, G.; Borghi, A. *Microchim. Acta* **2008**, *161*, 337−342.
(38) Gilmore, J. T. *Anal. Chem.* **1968**, *40*, 2230−2232.
(39) Margui, E.; Floor, G. H.; Hidalgo, M.; Kregsamer, P.; Roman-Ross, G.; Streli, C.; Queralt, I. *Anal. Chem.* **2010**, *82*, 7744−7751.
(40) Cahill, T. A. *Annu. Rev. Nucl. Part. Sci.* **1980**, *30*, 211−252.
(41) Iwanczyk, J. S.; Patt, B. E.; Barkan, S.; Feng, L.; Tull, C. R. *IEEE Trans. Nucl. Sci.* **2003**, *50*, 2470−2473.
(42) Raabe, O. G.; Braaten, D. A.; Axelbaum, R. L.; Teague, S. V.; Cahill, T. A. *J. Aerosol Sci.* **1988**, *19*, 183−195.
(43) Cahill, T. A.; Cahill, T. M.; Barnes, D. E.; Spada, N. J.; Miller, R. *Aerosol Sci. Technol.* **2011**, *45*, 1049−1059.